Journal of Mechanical Behavior of Biomedical Materials. **41**, pp. 325-335 (2015).
http://dx.doi.org/10.1016/j.jmbbm.2014.07.034

Characterization of persistent concussive syndrome using injury reconstruction and finite element modelling

Andrew Post[1] PhD, Marshall Kendall MSc[1], David Koncan MSc[1], Janie Cournoyer MSc[1], T. Blaine Hoshizaki[1] PhD, Michael D. Gilchrist[2,1] PhD, Susan Brien[3,1] MD, Michael D. Cusimano[4] MD, and Shawn Marshall[5] MD

Human Kinetics, University of Ottawa, Ottawa, Ontario, Canada[1]

School of Mechanical & Materials Engineering, University College Dublin, Dublin, Ireland[2]

Hull Hospital, Gatineau, Quebec, Canada[3]

St. Michael's Hospital, University of Toronto, Toronto, Ontario, Canada[4]

Ottawa General Hospital, Ottawa, Ontario, Canada[5]

Corresponding author: Andrew Post (apost@uottawa.ca) 200 Lees Ave., room A106, Ottawa, Ontario, Canada, K1N 6N5 – phone number: +1 (613)5625800 ext 7210

Key Words: Persistent concussive syndrome, brain injury, biomechanics, concussion

Abstract

Concussions occur 1.7 million times a year in North America, and account for approximately 75% of all traumatic brain injuries (TBI). Concussions usually cause transient symptoms but 10 to 20% of patients can have symptoms that persist longer than a month. The purpose of this research was to use reconstructions and finite element modeling to determine the brain tissue stresses and strains that occur in impacts that led to persistent post concussive symptoms (PCS) in hospitalized patients. A total of 21 PCS patients had their head impacts reconstructed using computational, physical and finite element methods. The dependent variables measured were maximum principal strain, von Mises stress (VMS), strain rate, and product of strain and strain rate. For maximum principal strain alone there were large regions of brain tissue incurring 30 to 40% strain. This large field of strain was also evident when using strain rate, product of strain and strain rate. In addition, VMS also showed large magnitudes of stress throughout the cerebrum tissues. The distribution of strains throughout the brain tissues indicated peak responses were always present in the grey matter (0.481), with the white matter showing significantly lower strains (0.380)($p<0.05$). The impact conditions of the PCS cases were severe in nature, with impacts against non-compliant surfaces (concrete, steel, ice) resulting in higher brain deformation. PCS biomechanical parameters were shown to fit between those that have been shown to cause transient post concussive symptoms and those that lead to actual pathologic damage like contusion, however, values of all metrics were characterized by large variance and high average responses. This data supports the theory that there exists a progressive continuum of impacts that lead to a progressive continuum of related severity of injury from transient symptoms to pathological damage.

1.0 Introduction

Concussive brain injuries resulting from impacts to the head are known to have serious short and long term effects (National Institutes of Health, 1999). In North America alone, an estimated 1.7 million concussions occur each year, accounting for approximately 75% of all traumatic brain injuries (TBI) (Bazarian et al., 2006). These injuries come with an estimated cost of over 60 billion $US, including health care costs as well as time away from work (Langlois et al., 2006). While most people who suffer concussions experience transient symptoms, some people suffer from persistent symptoms that last longer than three months. This long term symptomology of concussion is referred to as persistent post concussive syndrome (PCS) (National Institutes of Health, 1999; McCrory et al 2013). The significant impact PCS has on patients dictates the need to better understand the metrics that characterize the risk and severity of this brain injury. Brain injury reconstruction research has proposed peak linear and rotational acceleration and stress and strain parameters to characterize severity of injuries for those patients who experience transient concussive symptoms (King et al., 2003; Zhang et al., 2004; Kleiven, 2007), but no investigation has studied patients with PCS.

Currently, it is difficult, if not impossible to determine if a concussed individual will have a PCS injury. Even advanced neuroimaging with MRI is not able to predict which patient with a concussion will develop persistent symptoms. What is certain is that PCS, like other brain injuries, occurs through some form of injurious stress or strain applied to the brain tissue (Holbourn, 1943; Ommaya and Gennarelli, 1974; King et al., 2003; Kleiven, 2007; Post and Hoshizaki, 2012). This injurious loading can occur through contact (Wilinger and Baumgartner, 2003; Zhang et al., 2004; Kleiven, 2007), or through non-contact loading (Gennarelli et al., 1971; Ommaya and Genarelli, 1974). From a biomechanical perspective, brain injury, be it transient

concussion or PCS, is likely linked to the characteristics of the event that caused the injury (Post and Hoshizaki, 2012). These characteristics have been defined in the past as combinations of mass, velocity, location of impact, and others that determine the stresses and strains in the brain tissue (Post et al., 2012; Post et al., 2014; Karton et al., 2013). These brain injuries likely cause a complex series of cellular events that result in the symptomology associated with PCS (Giza and Hovda, 2001). A series of cellular events that for transient concussion is reversible, which is reflected by the short term symptomology. Morrison et al. (2000) correlated quantitative changes in gene expression in brain tissues of rats with mechanical stretch parameters. These changes are thought to be linked to concussive symptoms such as impaired coordination, attention, memory, and cognitive ability (Giza and Hovda, 2001). No definitive single gene expression has been linked to persistent symptoms after concussive injury. Shitaka et al. (2011) suggested the possibility of sustained activation of microglia for days to weeks after concussive injury to be partially responsible for persistent symptoms. Morrison et al., (2000) reported that the changes which occur following the mechanical impact of the brain could influence the severity of clinical outcome.

There has been some theories put forward suggesting that there is a continuum, or hierarchy, of brain injury (Hoshizaki et al., 2013; Post, 2013; Post et al., 2014). In the past researchers have shown that it is likely that no injury would be at the low ranges of head impact injury, followed by concussion, and finally TBI (Hoshizaki et al., 2013). However, recently there has been suggestions that within each of these brain injury categories (concussion and TBI) there is a further continuum that may be influenced by factors related not only to the increasing energy of impact, but to the characteristics of the event and how that affects the mechanisms of injury attached to particular anatomical structures (Hoshizaki et al., 2013; Post et al., 2014). While it is

likely that severity of impact may affect the occurrence of PCS, the characteristics leading to this type of injury have not been examined or in any way quantified. Further refinement of the theory of continuums of injury within concussion is important as it will help establish transient concussion and PCS as two separate injuries that may be related to different impact event characteristics. Once these differences are identified it would then be possible to refine the understanding of these types of injuries to permit for improved interventions and innovations based on prevention. Therefore, the purpose of this research was to use reconstructive techniques and finite element modelling to characterize brain injuries resulting in persistent concussive syndrome.

2.0 Methods:

Patients with PCS who were presented to one of three major urban hospitals in Canada were the subject population. Patients included in this research must have had accurate and complete eyewitness or personal accounts of the injury recorded by neurosurgeon that could be used in laboratory reconstructions. The description must have been complete enough to allow for estimation of the following criteria: head impact velocity, location, surface, and surface geometry. If there was no clear description of these parameters, the subject was excluded from the research dataset. In addition to these physical reconstruction parameters, CT and/or MRI images were taken of each patient to confirm no neurological lesion as confirmed by radiologist and neurosurgeon. In addition, to be classified as a PCS case, the subject must have had symptoms of concussion for a period lasting longer than four weeks. One thousand cases were examined for this research and 21 cases were found to be suitable for laboratory reconstruction.

The laboratory reconstruction of the PCS events were conducted by impacting a Hybrid III headform and neckform using a monorail drop rig or softball launcher depending on the

mechanism of injury for the event. The conditions (velocity, location, surface, surface geometry) as described by the Neurotrauma forms established the reconstructive parameters (Post, 2013). The Neurotrauma forms were hardcopy or electronic documents that were used as a standardized method to collect the impact parameters of the event for laboratory reconstruction purposes (Post et al., 2014; Post et al., 2014). These forms were filled in by the neurosurgeon or research assistant based on interviews with the patients involved. The information was then enhanced with information from the emergency rooms and paramedic reports. In the case of impact location on the headform, in all cases they were confirmed by scalp contusion that was visible by CT scan, confirming the contact site on the cranium. The impact velocity for falls was determined by conducting Mathematical Dynamic Models (MADYMO) simulations. The other cases involved walking/running, sit to stand, a kick to the head, a softball impact, and an impact from a falling wooden 2 x 6. The walking/running velocities were determined from the categories developed by DiMasio and Bradley (2013) based on the eyewitness assessments of the subject's speed. The sit to stand velocity was based on literature examining the normal and fast speed of this event for a normal population (Margaret et al., 2005). The kick to the head was conducted by a male of similar anthropometrics to the individual who conducted the kick to the head (section 2.1.5). The softball velocities were determined by using the average softball throwing velocities for the age of the thrower based upon Rojas II et al's research (2009). The wooden beam contact velocity was determined by the known height of the fall ($v=\sqrt{2gh}$). For each case, the Hybrid III headform was impacted three times.

2.1 Equipment

2.1.1 Monorail

To reconstruct the falling, collision, and sit to stand events a monorail drop rig device was used. This device was used for collisions because in all cases where a collision occurred it was head contact to immoveable objects. The Hybrid III headform was attached via a 50th Hybrid III neckform to the monorail by a drop carriage (Figure 1), permitting movement of the head in 6 degrees of freedom upon contact with the anvil. This attachment is similar to the Hybrid III full anthropometric dummy in that it allowed for some twisting rotation at the base of the neck but was likely limited by the stiffness of the rubber material, and thus representing a stiff neck condition. This is a limitation of the setup, but the linear and rotational accelerations from this type of experimental method have been shown to be within the range of human cadaveric response (Kendall et al., 2012). The drop carriage was attached to the monorail by ball bushings, which allowed low friction movement upon release. The release mechanism was a pneumatic piston. The anvil placed at the base of the monorail was changed to match the surface and geometry of the impact surface as described on the Neurotrauma report forms. Depending on the case, the impact surfaces were ice, concrete, wood, or steel. The impact velocity was determined by photoelectric time gate, which was positioned within 0.02 m of the impact.

Figure 1. Hybrid III attached to monorail with concrete anvil.

2.1.2 *Pneumatic ball launcher*

For projectile impacts (softball case) a pneumatic ball launcher was used to impact the Hybrid III headform (Figure 2). The pneumatic ball launcher consisted of two parts, the frame, which consisted of the air canister and launcher, and the table, which housed the Hybrid III headform.

The table (mass 12.78 ± 0.01kg) to which the Hybrid III head (mass 4.54 ± 0.01kg) and neckform (mass 1.54 ± 0.01kg) was attached was allowed to slide post impact. The post-impact sliding is necessary to preserve the equipment under high impact loading and occurs after the initial head contact has ended. An examination of the effect of sliding has been conducted in the laboratory and has been shown to have no effect on the resulting dynamic response. It also allowed for positioning of the Hybrid III headform so that the appropriate location would be impacted by the projectile. The impact velocity was determined by time gate at the muzzle of the pneumatic launcher. The impact site was first determined by laser target, and confirmed by high speed video of the event, collecting at 2000 fps.

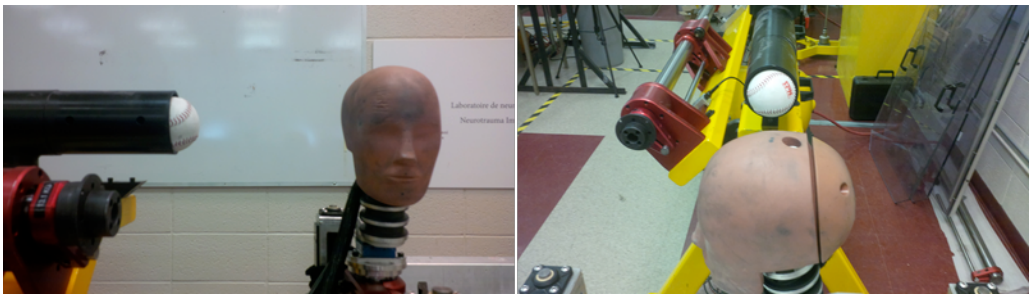

Figure 2.Hybrid III headform and pneumatic ball launcher.

2.1.3 Miscellaneous impacts

Two of the cases involved reconstructions that were not possible using standard fall/collision and projectile methodologies. Those were the kick to the head and the falling wooden 2 x 6 projectile impact. The kick to the head (Figure 3) was conducted by having a male participant of similar anthropometrics (5'10, 180 lbs) kick the Hybrid III headform that was placed in the same position as the injured person. In this case the person was prone; therefore the headform was attached by the Hybrid III neckform to a metal frame representing the body. This setup allowed for rotation and flexion of the head from the kick as was described by the eyewitness and subject.

The kick was applied using similar footwear to that from the event, and kick velocity was calculated from high speed camera recordings of the event.

Figure 3. Kick reconstruction.

The falling wooden 2 x 6 was reconstructed using the monorail. In this instance the subject was working and was impacted by the wooden 2 x 6 after it fell off a high shelf. To accomplish this reconstruction the 2 x 6 was hung by rope off a basket attached to the monorail with the Hybrid III headform attached to a metal frame by Hybrid III neckform in the impact zone. This allowed for the 2 x 6 to impact the Hybrid III in a way that was repeatable and realistic without adding any extra mass from the monorail system.

2.1.4 *Headform*

The headform impacted for this research was the Hybrid III 50th percentile anthropometric dummy headform (Figure 1). The neck used was also a Hybrid III neckform. The Hybrid III headform was equipped with a 3-2-2-2 accelerometer array to allow for the measurement of linear and rotational acceleration from the impact (Padgaonkar et al., 1975). The accelerometers used were Endevco 7264C-2KTZ-2-300 (Endevco, California, USA), and were sampled at 20 kHz. The data collection system used was a DTS TDAS systems and the data was filtered using a CFC class 1000 filter according to the SAE J211 convention for head impact data collection. This corresponds to a 1650 Hz lowpass (4-channel butterworth) filter that removes high

frequency vibrations from the impact to the headform. The reference system for the headform was x-axis forward, y-axis to the left of the head, and z-axis upwards.

2.1.5 *Mathematical Dynamic Models*

When head impact velocity was unclear from the information on Neurotrauma report forms, MADYMO (Tass International, Livonia, USA) simulations were conducted. For this dataset, these simulations were conducted for only the falling cases, as the other mechanisms had enough description to determine their approximate impact velocities. This software allows for the prediction of human kinematics for falls and pedestrian impacts in motor vehicle accidents. The MADYMO simulations were conducted based upon the initial body positions of the subject based on the Neurotrauma report form and the slip, or trip that resulted in the fall (Figure 4) (Adamec et al., 2010). A series of MADYMO simulations were conducted for each fall case to determine the upper and lower boundaries for velocity for the Hybrid III impact reconstructions (Post, 2013; Post et al., 2014).

Figure 4.MADYMO reconstruction of a trip on a curb.

2.2 Finite element model

The finite element model used in this study was the University College Dublin Brain Trauma Model (UCDBTM) (Horgan and Gilchrist, 2003, 2004). The geometry of the model was taken from a male cadaver using medical imaging techniques (Horgan and Gilchrist, 2003). The model

includes the scalp, skull, dura, CSF, pia, falx, tentorium, grey and white matter, cerebellum, and brain stem. Validation of the model was conducted, comparing the model response to intracranial pressure data from Nahum et al.'s (1977) cadaver impact tests and against brain motion using neutral density targets (NDT's) from Hardy et al.'s (2001) tests. Further validations were conducted via comparisons to real-world brain injury event reconstructions and simulations with good agreement (Doorly and Gilchrist, 2006).

Material parameters pertaining to the model are shown in Table and Table 2. The brain tissue was modelled using a linearly viscoelastic model combined with large deformation theory. The behaviour of this tissue was characterized as viscoelastic in shear with a deviatoric stress rate dependent on the shear relaxation modulus (Horgan and Gilchrist, 2003). Volumetric/hydrostatic compression of the brain tissue was considered elastic. The shear characteristics of the viscoelastic behaviour of the brain was expressed by:

$$(1) \quad G(t) = G_\infty + (G_0 - G_\infty)e^{-\beta t}$$

With G_∞ representing the long term shear modulus, G_0 the short term modulus and β is the decay factor. The Mooney-Rivlin hyperelastic material model was used for the brain to maintain these properties, in conjunction with a viscoelastic material property in ABAQUS, giving the material a decay factor of $\beta = 145\ s^{-1}$ (Horgan and Gilchrist, 2003). The hyperelastic law was given by:

$$(2) \quad C_{10}(t) = 0.9C_{01}(t) = 620.5 + 1930e^{-t/0.008} + 1103e^{-t/0.15}\ (\text{Pa})$$

where C_{10} is the mechanical energy absorbed by the material when the first strain invariant changes by a unit step input and C_{01} is the energy absorbed when the second strain invariant changes by a unit step (Mendis et al., 1995; Miller and Chinzei, 1997) and t is the time in seconds. The UCDBTM had a sliding boundary condition between the pia and CSF. This

algorithm allowed no separation of the contacting pia and CSF layers. Modelling of the CSF was done using solid elements with the bulk modulus of water and a low shear modulus (Horgan and Gilchrist 2003; Horgan and Gilchrist, 2004). For the sliding interfaces a friction coefficient of 0.2 was used (Miller et al., 1998).

Table 1 - Table of material properties for the University College Dublin Brain Trauma Model (Horgan and Gilchrist, 2003)

Material	Young's modulus (MPa)	Poisson's ratio	Density (kg/m^3)
Scalp	16.7	0.42	1000
Cortical Bone	15 000	0.22	2000
Trabecular Bone	1000	0.24	1300
Dura	31.5	0.45	1130
Pia	11.5	0.45	1130
Falx and Tentorium	31.5	0.45	1130
Brain	Hyper Elastic	0.499981	1060
CSF	15 000	0.5	1000
Facial Bone	500	0.23	2100

Table 2 - Material properties of brain tissue used in the University College Dublin Brain Trauma Model (Horgan, 2005)

	Shear modulus (kPa)		Decay constant (s^{-1})	Bulk modulus (GPa)
	G_0	G_∞		
Grey matter	10	2	80	2.19
White matter	12.5	2.5	80	2.19
Brain stem	22.5	4.5	80	2.19
Cerebellum	10	2	80	2.19

To ensure the validity of the finite element simulation, a model integrity check was conducted to examine the integrity of the solution based on the aspect ratio of the elements of the UCDBTM. The analyses were run to examine the distortion of the elements throughout the simulation time. Elements which showed large deformations (increase in aspect ratio greater than 1.0) in addition to being larger than 3:1 at time zero were identified and excluded from further analyses. This

threshold is based upon work conducted by Ho (2008) and Yang (2011). The results of these elements were excluded as upon examination were found to be the result of impossible geometries resulting in high strains (due to high aspect ratios). All of elements which were eliminated were found to be along the tentorium and falx membranes. In total, 217 elements were excluded in these regions, which is less than 1% of the total elements of the UCDBTM. The remaining elements were all found to have aspect ratios under 3:1 and demonstrated normal loading conditions from the input dynamic response time histories.

2.3 Statistics

A comparison of the peak maximum principal strain, von Mises stress, strain rate, and product of strain and strain rate in the grey and white matter was run using a paired t-test with significance level set to 0.05.

3.0 Results:

Twenty one PCS cases were analyzed covering three mechanisms of injury (11 falls, 8 collisions, 2 projectiles). Case descriptions and impact locations are presented in figure 5 and table 3 with the results in figures 6 through 9, and table 4. For these PCS reconstructions, the average peak maximum strain was found to occur in the grey matter of the cerebrum (0.483), with significantly lower strains in the white matter (0.380)($p<0.05$).

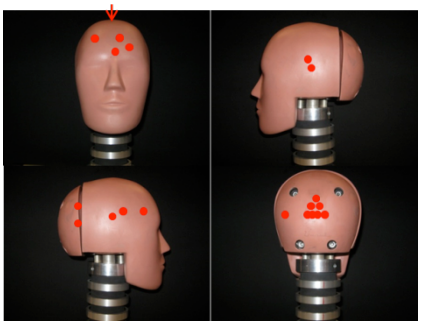

Figure 5.Impact locations for the PCS cases.

ıble 3 - Case descriptions with impact surface, velocity and location

ase	Mechanism	Gender	Age	Velocity (m/s)	Impact location	Equipment Used	Velocity Sources of Estimates
1	Fall – Ice	F	62	3.6 - 6.6	Back of head	Monorail	Madymo
2	Collision – Rubber sole of shoe	F	31	17.7 - 21.9	Right occiput	Kick	High speed camera
3	Fall – Ice	M	37	4.9 - 5.4	Left side of head	Monorail	Madymo
4	Collision – Wood truss	F	41	0.6 - 2.0	Bridge of nose	Pendulum	DiMascio et al., (2013)
5	Fall – Concrete	F	59	3.7 - 6.1	Right Occiput	Monorail	Madymo
6	Fall – Concrete	M	58	4.7 - 5.7	Back of head	Monorail	Madymo
7	Fall – Concrete	F	54	4.0 - 4.8	Right medial parietal region	Monorail	Madymo
8	Fall – Concrete	F	51	3.2 - 3.6	Back of head	Monorail	Madymo
9	Fall – Ice	F	52	3.8 - 6.6	Upper right occiput	Monorail	Madymo
10	Fall – Concrete	F	65	3.7 - 6.1	Posterior aspect of skull, occipitoparietal region	Monorail	Madymo
11	Projectile – Softball	F	35	15.0 - 25.0	Left temporal region	Ball Launcher	Rojas et al., (2009)
12	Collision – Concrete staircase	M	41	4.0 - 5.5	Forehead	Monorail	DiMascio et al., (2013)
13	Fall – Concrete	M	52	3.1 - 5.6	Left side of face and eye	Monorail	Madymo
14	Fall – Concrete	F	57	3.8 - 6.7	Occiput	Monorail	Madymo
15	Fall – Concrete	M	49	3.8 - 6.3	Occiput	Monorail	Madymo
16	Projectile – 2x6 wood beam	F	50	7.0 - 9.1	Left temple	Monorail	Height of fall
17	Collision – Wood truss	M	44	0.6 - 0.9	Vertex of skull	Monorail	Margaret et al., (2005)

18	Collision – Steel sign	M	48	0.2 - 2.0	Left side of head	Monorail	DiMascio et al., (2013)
19	Collision – Wood truss	F	50	4.0 - 5.5	Crown of head	Monorail	DiMascio et al., (2013)
20	Collision – Wood truss	F	39	1.5 - 1.7	Back of head	Monorail	Margaret et al., (2005)
21	Collision – Steel table leg	F	55	3.8 - 4.2	Right frontal area	Monorail	DiMascio et al., (2013)

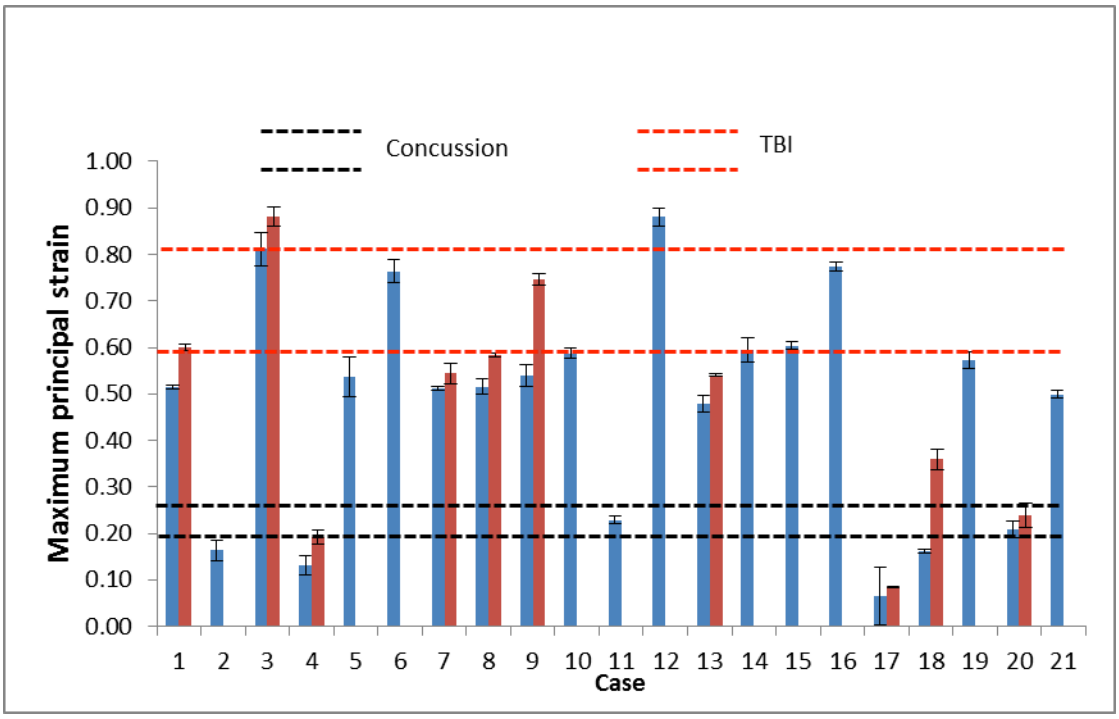

Figure 6. Cerebrum maximum principal strain responses for the PCS cases. Suggested ranges of concussion from the literature represented by black dotted lines (Zhang et al., 2004; Kleiven, 2007), ranges of TBI represented by red dotted lines (Doorly, 2007; Post, 2013).

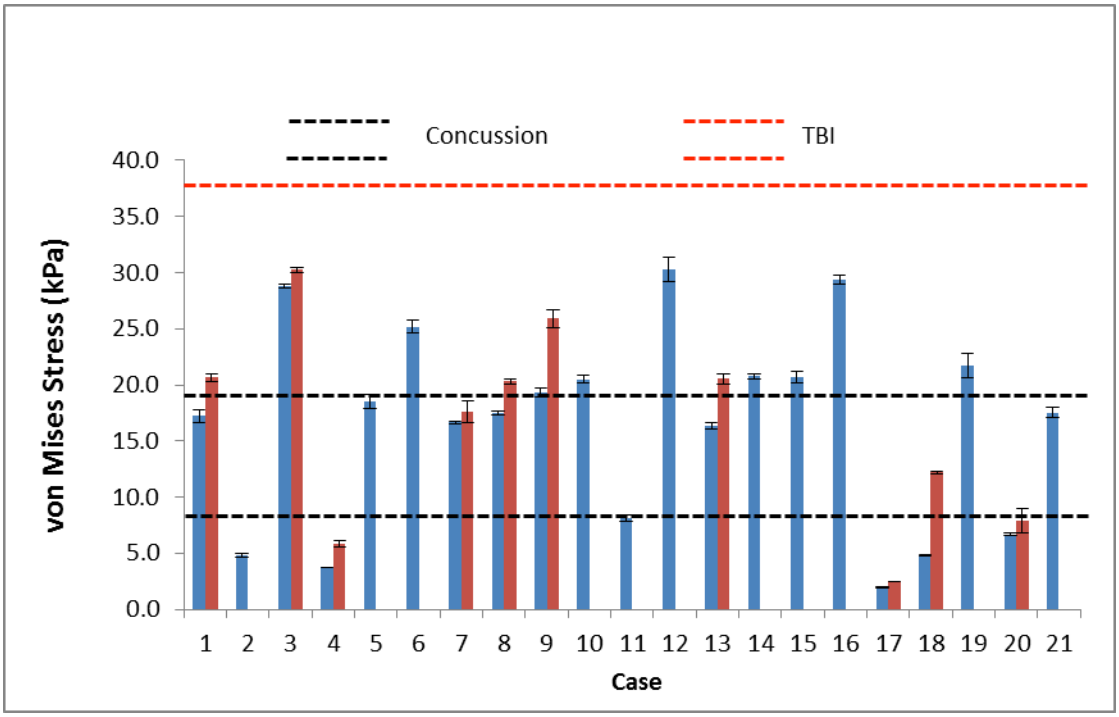

Figure 7. Cerebrum von Mises stress responses for the PCS cases. Suggested ranges of concussion from the literature represented by black dotted lines (Zhang et al., 2004; Willinger and Baumgartner, 2003; Kleiven, 2007), ranges of TBI represented by red dotted lines (Doorly, 2007; Post 2013).

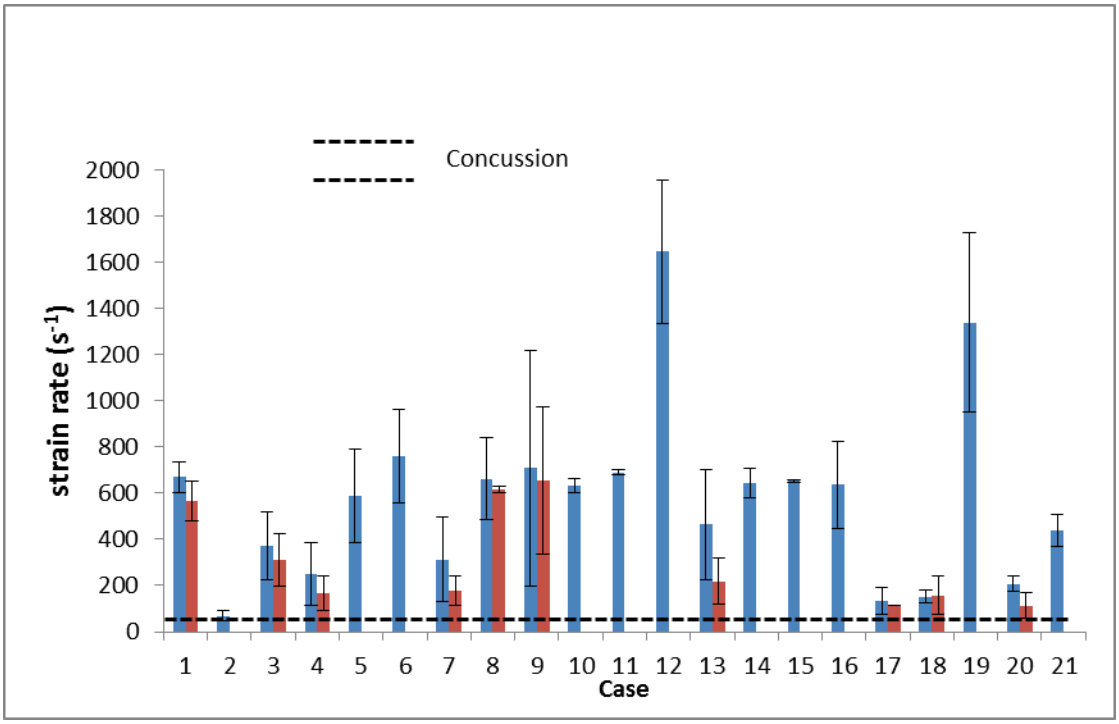

Figure 8. Cerebrum strain rate responses for the PCS cases. Suggested ranges of concussion from the literature represented by black dotted lines (King et al., 2003; Kleiven, 2007), no cerebral TBI values available.

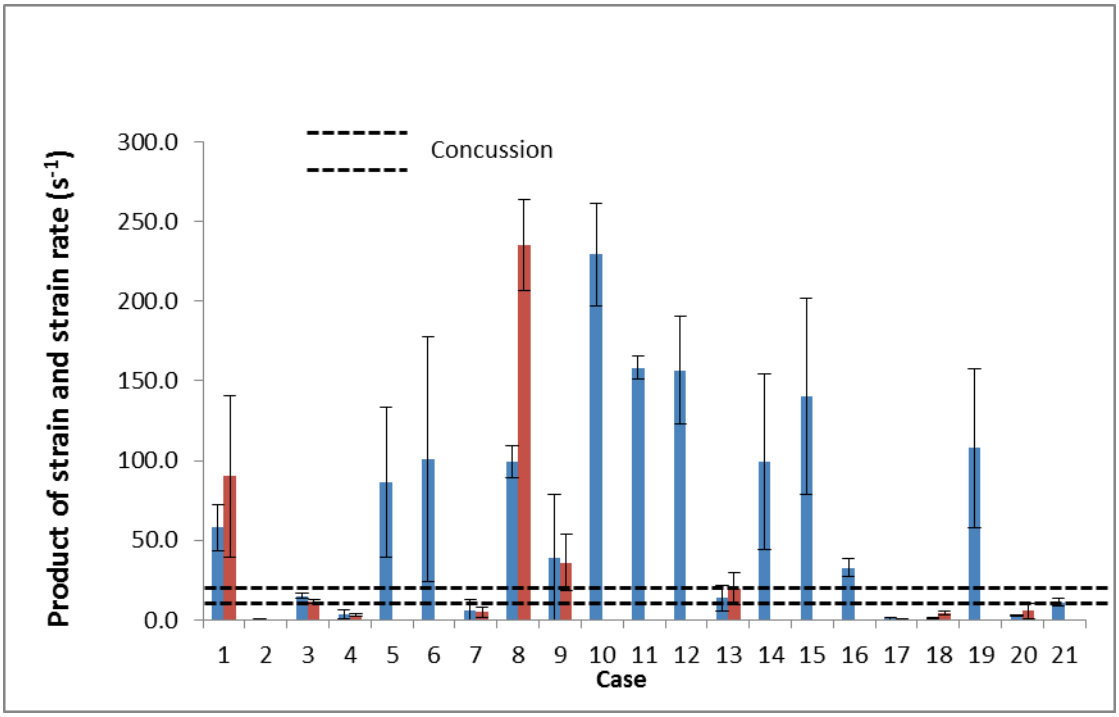

Figure 9. Cerebrum product of strain and strain rate responses for the PCS cases. Suggested ranges of concussion from the literature represented by black dotted lines (King et al., 2003; Kleiven, 2007), no cerebral TBI values available.

Table 4 - Averaged finite element responses including region specific strains

	Impact Velocity (m/s)	Peak Maximum Principal Strain	Strain in Grey Matter	Strain in White Matter	Peak Strain Rate (s^{-1})	Product of Strain and Strain Rate (s^{-1})	Peak Von Mises Stress (kPa)
Average	3.2	0.483	0.483	0.380	573.0	64.8	16.7
SD	1.7	0.237	0.236	0.191	377.3	66.7	8.6

4.0 Discussion

The reconstructions of PCS hospital cases were represented by three mechanisms of injury: falls, collisions, and projectiles. None of the cases experienced mechanical failure as evidenced by the

normal CT and/or MRI for each subject, but all showed PCS. In general, these cases were characterized by low (0.2 m/s) to high (15 m/s) impact velocities (3.2 m/s average) with relatively non-compliant surfaces such as concrete, ice, steel, and wood. There was a range of responses, highlighted by the large standard deviations across all brain deformation metrics. This phenomenon is a result of the varying mechanisms of injury that caused the resulting PCS injury. In this study, the data was treated as one complete set as described by the endpoint injury (in this case PCS), while it is likely that each mechanism has particular characteristics that would create a substantial risk of PCS. For example, all the fall cases were characterized by high magnitude stresses and strains, many caused by slips and falls onto concrete or other unyielding surface. The projectile impacts were unique events which also caused high stresses and strains, but this was accomplished through higher velocities that resulted in a shorter acceleration time histories (<5 ms). The collisions were also caused by impacts to non-compliant surfaces, but generally at lower velocities (under 3.8 m/s). Of all the cases there were five that resulted in magnitudes of stress and strain that were less than those expected for concussion (cases 2,3,17,18, and 20) (King et al., 2003; Zhang et al., 2004). The varied nature of the impact conditions in these cases suggest that it is possible that pure biomechanics of impact may not be fully descriptive of the risk for these individual cases and perhaps they had a susceptibility to incurring a concussive or PCS injury.

In comparison with the current literature on concussive thresholds, these PCS hospital cases show results consistent with previous research (Table 5) (Zhang et al., 2004; Kleiven 2007; Willinger and Baumgartner 2003). This data set of PCS reconstructions were characterized by a large variance in resultant metrics, with large magnitude brain stress and strain responses, far larger than would be expected based on previous concussion literature (King et al., 2003; Zhang

et al., 2004). As a result, this research would suggest that higher stresses and strains are representative of PCS injury in the UCDBTM. In addition, it is likely that these stresses and strains may be representative of the presence of a more severe injury; ones that may lead to the physiological cascades producing the symptomology of concussion (Giza and Hovda 2001) by many different potential mechanisms including: 1) a complex series of ionic, metabolic, and other physiologic changes take place that contribute to the persistent symptoms (Giza and Hovda, 2001), 2) to changes in gene expression (Morrison et al. 2000), 3) to sustained activation of microglia for days to weeks Shitaka et al. (2011), or 4) other mechanisms.

Though there are no clear patterns in metrics when comparing to thresholds of concussive injury, when comparing the location of maximum principal strain in the cerebrum, the maximum magnitudes were incurred in the grey matter of the brain in all cases. These results are consistent with work conducted by Kleiven (2007), who found peak strains in the grey matter to be a possible predictor of concussion resulting from impact reconstructions of NFL concussion cases. Since symptoms of concussion often include cognitive dysfunction, any excessive strain in the cognitive centers in the grey matter may also be influential in the presence of concussive symptoms (Zhang et al., 2004). Furthermore, persistence of symptoms has been linked to abnormalities in grey matter following strains from TBI (Shitaka et al., 2011), supporting that excessive strain in grey matter might influence persistence of symptoms. It should be noted that the UCDBTM and other finite element models characterize the modulus for the grey matter lower than that for the white matter. This would result in the grey matter often demonstrating higher strains than the white matter, as it would have a softer response. While these material parameters were derived from cadaveric testing and have been considered to have a reasonable

transferability to human responses, the effect of the characterization of the brain tissues on the results should be considered when interpreting the results.

Table 5 - Concussion thresholds created from finite element responses of real-world accident reconstructions

Concussion threshold value (50% chance)	Dependent variable	Location	Reference
0.21	Maximum Principal Strain	Corpus Callosum	Kleiven (2007)
0.26	Maximum Principal Strain	Grey Matter	Kleiven (2007)
0.19	Maximum Principal Strain	Grey Matter	Zhang et al. (2004)
48.5 s^{-1}	Strain rate	Grey Matter	Kleiven (2007)
60 s^{-1}	Strain rate	Brain	King et al. (2003)
10.1 s^{-1}	Product of Strain and Strain rate	Grey Matter	Kleiven (2007)
19 s^{-1}	Product of Strain and Strain rate	Brain	King et al. (2003)
8.4 kPa	Von Mises Stress	Corpus Callosum	Kleiven (2007)
7.8 kPa	Von Mises Stress	Brain Stem	Zhang et al. (2004)
18 kPa	Von Mises Stress	Brain	Willinger and Baumgartner (2003)

In many cases the stresses and strains for PCS are much higher than concussive thresholds with many falling within the ranges more characteristic of impacts that lead to pathological lesions like contusion or subdural hematoma rather than concussion (Table 6). When conducting a comparison to these thresholds, it is important to note that they were created using finite element responses from the region of injury rather than peak strain reached in the cerebrum, as presented here. In comparison to previous research involving mechanisms of TBI, Post (2013) conducted reconstructions of 20 cases of patients with TBI with peak strains in the cerebrum averaging 0.810. In addition, Doorly (2007) reconstructed 10 cases of TBI, with peak strains in the cerebrum reaching 0.599. Both of these studies were conducted using the UCDBTM, showing that higher cerebral strain values characteristic of TBI are often larger than those of the PCS

cases presented here (0.483 average). The data presented in this research data indicates that PCS cases may fit between those impacts that lead to transient concussive symptoms (King et al., 2003; Willinger and Baumgartner, 2003; Zhang et al., 2004; Kleiven, 2007), and those that lead to TBI (Doorly 2007; Post, 2013). The present research supports the theory that there may be a continuum of injuries ranging from concussion with transient symptoms, to PCS, and finally TBI (Hoshizaki et al. 2013).

Table 6- Specific TBI thresholds using finite element responses from accident-reconstructions (Doorly and Gilchrist, 2006;Doorly, 2007)

Threshold for injury	Dependent variable	Injury type
0.14 - 0.53	Maximum Principal Strain	Subdural hematoma
5 - 17 kPa	Von Mises Stress	Subdural hematoma
147 - 348 s^{-1}	Strain rate	Subdural hematoma
14 - 24 s^{-1}	Product of Strain and Strain rate	Subdural hematoma
0.16 - 0.23	Maximum Principal Strain	Contusion
5 - 8 kPa	Von Mises Stress	Contusion
119 - 265 s^{-1}	Strain rate	Contusion
14.7 - 56.3 s^{-1}	Product of Strain and Strain rate	Contusion
0.34	Maximum Principal Strain	Subarachnoid hemorrhage
12.2 kPa	Von Mises Stress	Subarachnoid hemorrhage
197 s^{-1}	Strain rate	Subarachnoid hemorrhage
36.3 s^{-1}	Product of Strain and Strain rate	Subarachnoid hemorrhage
0.16 - 0.23	Maximum Principal Strain	Epidural hematoma
4.8 - 7.9 kPa	Von Mises Stress	Epidural hematoma
129 - 141 s^{-1}	Strain rate	Epidural hematoma
14.5 – 19.0 s^{-1}	Product of Strain and Strain rate	Epidural hematoma

5.0 Conclusion

These reconstructions of PCS showed brain tissue stresses and strains higher than those previously reported in concussions with transient symptoms. These higher stresses and strains may be indicative of the magnitudes required to incur pathophysiological responses that lead to PCS. The impacts were characterized by impact velocities ranging from 0.2 - 4.7 m/s onto low-compliance surfaces (two projectile cases were higher velocity). In every case, the peak strain value was found in the grey matter, which is consistent with previous literature investigating mechanisms of concussive injury. Overall, this data set supports a continuum of injury theory as proposed by Hoshizaki et al. (2013), with average values for PCS fitting in between transient concussions and TBI on a scale of severity when using global cerebrum responses.

5.1 Limitations

These cases represent one source of PCS injuries, which could be considered severe as they were presented at hospital emergency rooms. Helmeted sports are another common source of PCS injuries and are not represented by this dataset. It is likely that sports are characterized by differing and unique characteristics that contribute to a likelihood of PCS. For example, significant differences between hospital and sports data sets could be the protective equipment and impact velocities in which the injuries are sustained (Hoshizaki et al., 2013). The limitations of this study pertain to both accident reconstructions and the finite element model.For reconstructive purposes, assumptions are made regarding impact velocity, vector, and surfaces. These parameters are replicated as close to the original impact as possible however there remains a small margin of error. Additionally, the Hybrid III headform is not biofidelic in its response but still gives a good representation of the accelerations experienced during impact. The monorail drop method for reconstructing falls has been used in the past to research TBI and does not include a representation of the inertial effects of the torso. These effects may be in some way

mitigated by the compliance of the neck, but would have some influence on the resulting dynamic response. These assumptions and limitations can affect the end parameters of brain stresses/strains. There are also limitations associated with any finite element model, with assumptions on boundary conditions, and material properties. The UCDBTM is used as an approximation of the response of the brain under load, using tissue characteristics and validated responses of cadavers comparable to other finite element models. Although validated, the true response of the brain is still unknown and for this reason, the response of the model may not reflect the response of brain under loading. In addition to material characteristics, the hyperelastic material model which is employed will also influence the results as a change in material model will likely change the response. The geometry of the model is also based on CT and MRI images of one subject and so does not reflect individual differences between cases. The results are also limited by the cases that met our inclusion criteria and future research should aim to replicate our findings with larger numbers of patients.

Acknowledgement

Canadian Brain Injury and Violence Research Team

6.0 References

Adamec, J., Jelen, K., Kubovy, P., Lopot, F., & Schuller, E. (2010). Forensic biomechanical analysis of falls from height using numerical human body models. *Journal of Forensic Science, 55(6),* 1615-1623.

Bazarian, J. J., Veazie, P., Mookerjee, S., & Lerner, B. (2006). Accuracy of mild traumatic brain injury case ascertainment using ICD-0 codes. *Academic Emergency Medicine, 13*, 31-38.

Dimasio, M., & Bradley P., (2013). Evaluation of the most intense high-intensity running speed in English FA Premier League soccer matches. *Journal of Strength & Conditioning Research*, 27(4), 909-915.

Doorly, M. C. (2007). *Investigations into head injury criteria using numerical reconstruction of real life accident cases.* (PhD, University College Dublin).

Doorly, M. C., & Gilchrist, M. D. (2006). The use of accident reconstruction for the analysis of traumatic brain injury due to head impacts arising from falls. *Computer Methods in Biomechanics and Biomedical Engineering, 9*(6), 371-377.

Gennarelli, T. A., Ommaya, A. K., & Thibault, L. E. (1971).Comparison of translational and rotaional head motions in experimental cerebral concussion. *15th Stapp Car Crash Conference,* 797-803.

Giza, C., & Hovda, D. (2001).The neurometabolic cascade of concussion. *Journal of Athletic Training, 36*(3), 228-235.

Hardy, W. N., Foster Craig D., Mason, M. J., Yang, K. H., King, A. I., &Tashman, S. (2001). Investigation of head injury mecahnisms using neutral density technology and high-speed biplanar X-ray. *Stapp Car Crash Journal, 45*, 337.

Ho, J. (2008). *Generation of patient specific finite element models*. (PhD, Royal Institute of Technology, Sweden)

Holbourn, A.H.S. (1943). Mechanics of head injuries. *Lancet*.

Horgan, T. J., & Gilchrist, M. D. (2003).The creation of three-dimensional finite element model for simulating head impact biomechanics. *International Journal of Crashworthiness, 8*(4), 353.

Horgan, T. J., & Gilchrist, M. D. (2004). Influence of FE model variability in predicting brain motion and intracranial pressure changes in head impact simulations. *International Journal of Crashworthiness, 9*(4), 401-418.

Hoshizaki, T., Post, A., Kendall, M., Karton, C., & Brien, S. (2013). The relationship between head impact characteristics and brain trauma. *Journal of Neurology & Neurophysiology, 5*(1), 181.

Karton C., Hoshizaki T.B. and Gilchrist M.D., (2013). The influence of inbound mass on the dynamic impact response of the Hybrid III headform and tissue deformation response characteristics. *Journal of ASTM international,* DOI: 10.1520/STP155220120175

Kendall, M., Post, A., Rousseau, P., Oeur, A., Gilchrist, M.D., & Hoshizaki, T.B., (2012). A comparison of dynamic impact response and brain deformation metrics within the cerebrum of head impact reconstructions representing three mechanisms of head injury in ice hockey. *Proc. IRCOBI conference*, Dublin, Ireland.

King, A. I., Yang, K. H., Zhang, L., Hardy, W. N., &Viano, D. C. (2003). Is head injury caused by linear or angular acceleration? *IRCOBI Conference,* Lisbon, Portugal.

Kleiven, S. (2007). Predictors for traumatic brain injuries evaluated through accident reconstructions. *Stapp Car Crash Journal, 51*, 81-114.

Langlois, J. A., Rutland-Brown, W., & Wald, M. (2006). The epidemiology and impact of traumatic brain injury: A brief overview. *Journal of Head Trauma Rehabilitation, 21*(5), 375-378.

Margaret, K.Y., Mak C., & Hui-Chan W.Y., (2005). The speed of sit-to-stand can be modulated in Parkinson's disease. *Clinical Neuropsychology, 116(4),* 780-789.

Mendis, K.K., Stalnaker, R.L., & Advani, S.H., (1995). A constitutive relationship for large deformation finite element modeling of brain tissue. *Transactions of the ASME Journal of Biomedical Engineering, 117*, 279-285.

Miller, K., & Chinzei, K., (1997). Constitutive modelling of brain tissue: Experiment and theory. *Journal of Biomechanics, 30(11),* 1115-1121.

Miller, R., Margulies, S. S., Leoni, M., Nonaka, M., Chen, X., Smith, D., &Meaney, D. F. (1998). Finite element modeling approaches for predicting injury in an experimental model of severe diffuse axonal injury. *42nd Stapp Car Crash Conference,* Arizona. 155-166.

McCrory, P., Meeuwisse, W.H., Aubry, M., Cantu, B., Dvorak, J., Echemendia, R.J., et al. (2013). Consensus statement on concussion in sport: the 4th international conference on concussion in sport held in Zurich, Nov 2012. *British Journal of Sports Medicine, 47*, 250-258.

Morrison, B., Meaney, D. F., Margulies, S. S., & McIntosh, T. (2000). Dynamic mechanical stretch of organotypic brain slice cultures induces DIfferential genomic expression: Relationship to mechanical parameters. *Journal of Biomechanial Engineering, 122*, 224-230.

Nahum, A. M., Smith, R., & Ward, C. (1977).Intracranial pressure dynamics during head impact. *21st Stapp Car Crash Conference,* Warrendale, PA. 337.

National Institutes of Health.(1999). Rehabilitation of persons with traumatic brain injury. *Journal of the American Medical Association, 282*(10), 974-983.

Ommaya, A. K., & Gennarelli, T. A. (1974). Cerebral concussion and traumatic unconsciousness: Correlation of experimental and clinical observations on blunt head injuries. *Brain, 97*, 633-654.

Padgaonkar, A. J., Krieger, K. W., & King, A. I. (1975).Measurement of angular acceleration of a rigid body using linear accelerometers. *Journal of Applied Mechanics, 42*(3), 552-556.

Post, A. (2013). *The influence of dynamic response characteristics on traumatic brain injury.* (PhD, University of Ottawa).

Post, A., & Hoshizaki, T.B. (2012) Mechanical properties describing brain impact injuries: A review. *Trauma, 14(4),* 327-349.

Post, A., Hoshizaki, T.B., Gilchrist, M.D., Brien, S., Cusimano, M., Marshall, S. (2014). The influence of dynamic response and brain deformation metrics on the occurrence of subdural hematoma in different regions of the brain. *Journal of Neurosurgery, 120(2)*, 453-461.

Rojas, I., Provencher, M., Bhatia, S., Foucher, K., Bach Jr, B., Romeo, A., Wimmer, M., & Verma, N., (2009). Biceps activity during windmill softball pitching. *American Journal of Sports Medicine, 37(3),* DOI: 10.1177/0363546508328105.

Shitaka, Y., Tran, H. T., Bennett, R., E., Sanchez, L., Levy, M. A., Dikranian, K., & Brody, D. L. (2011). Repetitive closed-skull traumatic brain injury in mice causes persistent multifocal axonal injury and microglial reactivity. *Journal of Neuropathology and Experimental Neurology, 70*(7), 551-567.

Willinger, R., & Baumgartner, D. (2003). Human head tolerance limits to specific injury mechanisms. *International Journal of Crashworthiness, 8*(6), 605-617.

Yang, J., (2011). Investigation of brain trauma biomechanics in vehicle traffic accidents using human body computational models. In Wittek, A., Nielsen, P.M.F., and Miller, K. (eds), Computational Medicine: Soft Tissues and the Musculoskeletal system, New York, Springer, pp 5-14.

Zhang, L., Yang, K. H., & King, A. I. (2004). A proposed injury threshold for mild traumatic brain injury. *Journal of Biomechanial Engineering, 126*, 226-236.